

Immobilized Metal Complexes in Porous Organic Hosts: Development of a Material for the Selective and Reversible Binding of Nitric Oxide

Karen M. Padden,[†] John F. Krebs,[†] Cora E. MacBeth,[†] Robert C. Scarrow,[‡] and A. S. Borovik^{*,†}

Contribution from the Departments of Chemistry, University of Kansas, Lawrence, Kansas 66045, and Haverford College, Haverford, Pennsylvania 19041-1392

Received September 5, 2000

Abstract: Delivery of NO to specific targets is important in fundamental studies and therapeutic applications. Various methods have been reported for delivery of NO in vivo and in vitro; however, there are few examples of systems that reversibly bind NO. Reported herein is the development of a new polymer (P-1[Co^{II}]) that reversibly binds NO. P-1[Co^{II}] has a significantly higher affinity for NO compared to O₂, CO₂, and CO. The polymer is synthesized by template copolymerization methods and consists of a porous methacrylate network, containing immobilized four-coordinate Co^{II} sites. Binding of NO causes an immediate color change, indicating coordination of NO to the site-isolated Co^{II} centers. The formation of P-1[Co(NO)] has been confirmed by EPR, electronic absorbance, and X-ray absorption spectroscopies. Electronic and X-ray absorbance results for P-1[Co^{II}] and P-1[Co(NO)] show that the coordination geometry of the immobilized cobalt complexes are similar to those of their monomeric analogues and that NO binds directly to the cobalt centers. EPR spectra show that the binding of NO to P-1[Co^{II}] is reversible in the solid state; the axial EPR signal associated with the four-coordinate Co^{II} sites in P-1[Co^{II}] is quenched upon NO binding. At room temperature and atmospheric pressure, 40% conversion of P-1[Co(NO)] to P-1[Co^{II}] is achieved in 14 days; under vacuum at 120 °C this conversion is complete in ~1 h. The binding of NO to P-1[Co^{II}] is also observed when the polymer is suspended in liquids, including water.

Introduction

The design and synthesis of a new polymeric material that reversibly binds nitric oxide (NO) is reported. The polymer contains discrete metal sites with a high affinity for NO. It is composed of isolated four-coordinate Co^{II} complexes immobilized in a highly cross-linked and porous methacrylate host. An important consequence of the NO binding event is a rapid and vivid color change of the material from orange to dark brown-green. This dramatic color change leads to immediate confirmation of the presence of nitric oxide in gas and solution phases. Moreover, the immobilized Co^{II} sites have a significantly greater affinity for NO over other biologically important gaseous compounds such as O₂, CO₂, and CO.

Interest in the chemistry of NO has intensified in recent years because of its proposed role in numerous physiological functions.¹ The multifaceted biological importance of NO can be separated into three categories including protective, regulatory, and deleterious.² Protective effects include nitric oxide as an antioxidant agent and inhibitor to leukocyte adhesion. Among the many regulatory effects of NO are its ability to control vascular tone and permeability, cellular adhesion, and renal function. Nitric oxide has also been established as a neurotransmitter, bronchodilator, and inhibitor of platelet aggregation. In addition, data strongly suggest that NO is the final common effector molecule of nitrovasodilators, which activate soluble

guanylyl cyclase. Nitric oxide also has several deleterious effects, including inhibiting enzyme function, as well as inducing DNA damage and lipid peroxidation.^{3,4}

It is evident from the varied biological effects listed above that both the release and scavenging of nitric oxide are desirable under physiological conditions. A variety of different systems have been reported to dispense NO. The simplest cases use direct inhalation of NO, which has been effective in reversing pulmonary hypertension.⁵ Organic compounds have been developed that release NO via decomposition routes. For example, anionic diazeniumdiolates⁶ dissociate in a first-order reaction at constant pH to produce 2 equiv of NO. This class of compounds has shown promise as prodrugs for protection of cells from free radical mediated toxicity² and for the relaxation of vascular smooth muscle cells.⁶ Dispensing NO via photorelease mechanisms has also been explored; recent examples include the photorelease of NO from nitrosothiol-derivatized surfaces,⁷ Roussin's salts,⁸ Fe–NO porphyrins,⁹ and Cr^{III}–nitrite complexes.¹⁰

(3) Culotta, E.; Koshland, D. E. *Science* **1992**, *258*, 1862–1865.

(4) Ignarrow, L. J. *Pharm. Res.* **1989**, *6*, 651–659.

(5) Rossaint, R.; Falke, K. J.; López, F.; Slama, K.; Pison, U.; Zapol, W. M. *N. Engl. J. Med.* **1993**, *328*, 399–405.

(6) For example see: Keefer, L. K.; Nims, R. W.; Davies, K. M.; Wink, D. A. *Methods Enzymol.* **1996**, *268*, 281–293.

(7) Etchenique, R.; Furman, M.; Olabe, J. A. *J. Am. Chem. Soc.* **2000**, *122*, 3967–3968.

(8) Bourassa, J.; DeGraff, W.; Kudo, S.; Wink, D. A.; Mitchell, J. B.; Ford, P. C. *J. Am. Chem. Soc.* **1997**, *119*, 2853–2860.

(9) Hoshino, M.; Ozawa, K.; Seki, H.; Ford, P. C. *J. Am. Chem. Soc.* **1993**, *115*, 9568–9575.

(10) De Leo, M.; Ford, P. C. *J. Am. Chem. Soc.* **1999**, *121*, 1980–1981.

[†] University of Kansas.

[‡] Haverford College.

(1) For examples see: Moncada, S.; Palmer, R. M. J.; Higgs, E. A. *Pharmacol. Rev.* **1991**, *43*, 109–142.

(2) Wink, D. A.; Mitchell, J. B. *Free Radical Biol. Med.* **1998**, *25*, 434–456.

While there have been many advances in the technology of NO delivery, there are few examples of systems that have the capability to reversibly bind NO.^{10,11} Useful applications exist both in vivo and in vitro for materials that store and subsequently release NO. Furthermore, a durable material that readily scavenges NO would have important applications in cases where high NO concentrations could lead to detrimental effects, such as DNA damage. We have recently shown that immobilized metal complexes in porous organic hosts can serve as sites for the reversible binding of CO¹² and O₂.¹³ These materials are formed by template copolymerization methods, a technique that is used in making molecularly imprinted polymers.¹⁴ Materials made in this way have a significant number of metal sites (~90%) that are isolated from each other by a porous host.¹⁵ Site isolation of the metal complexes is advantageous because the formation of undesirable bimolecular metal-based adducts is prevented and the function of the polymer is prolonged.

This copolymerization method has been used to develop P-1[Co^{II}], a material that binds NO to form P-1[Co(NO)]. Spectroscopic measurements confirm that NO binding occurs at coordinatively unsaturated Co^{II} sites, which are monodispersed within the porous host. The NO-loaded polymer, P-1[Co(NO)], is stable in the solid state at 25 °C for days. However, slow loss of NO from P-1[Co(NO)] is observed at room temperature with a 40% loss of NO occurring after 14 d. The release rate of NO can be accelerated by increasing temperature with a maximum loss observed within ~1 h/50 mg of polymer, after heating at 120 °C under vacuum. The recovered polymer retains affinity for binding NO.

Experimental Section

Solvents and reagents were used as received from either Fisher or Aldrich unless otherwise noted. Solvents used under an inert atmosphere for synthesis or sample preparation were dried following standard procedures.¹⁶ Ethylenediamine and 3,3'-diamino-*N*-methylpropylamine were distilled under nitrogen immediately before use. Co(OAc)₂·4H₂O was dehydrated by heating to 120 °C under vacuum for 48 h.

Synthesis of some complexes and preparation of polymerization reactions were conducted in a Vacuum Atmospheres drybox under an argon atmosphere. Standard Schlenk techniques were used during the workup of some reactions and manipulations of polymer samples outside the drybox. Elemental analyses were conducted by either Desert Analytics (Tucson, AZ), the University of Kansas Department of Medicinal Chemistry MicroLab, or the analytical services laboratory of the Department of Animal Sciences at Kansas State University. The compounds 2-hydroxy-4-(4-vinylbenzylmethoxy)benzaldehyde¹⁷ and bis[2-hydroxy-4-(4-vinylbenzylmethoxy)benzaldehyde]ethylenediimine (H₂I)^{15,18} were synthesized following literature methods.

(11) (a) Ribeiro, J. M. C.; Hazzard, J. M. H.; Nussenzveig, R. H.; Champagne, D. E.; Walker, F. A. *Science* **1993**, *260*, 539–541. (b) Ding, X. D.; Weichsel, A.; Andersen, J. F.; Shokhireva, T. K.; Balfour, C.; Pierik, A. J.; Averill, B. A.; Montfort, W. R.; Walker, F. A. *J. Am. Chem. Soc.* **1999**, *121*, 128–138 and references therein.

(12) (a) Krebs, J. F.; Borovik, A. S. *J. Am. Chem. Soc.* **1995**, *117*, 10593–10594. (b) Krebs, J. F.; Borovik, A. S. In *Molecular and Ionic Recognition with Imprinted Polymers*; ACS Symp. Ser. No. 703; Bartsch, R. A., Maeda, M., Eds.; American Chemical Society: Washington, DC, 1998; pp 159–170.

(13) Krebs, J. F.; Borovik, A. S. *Chem. Commun.* **1998**, 553–554.

(14) (a) Wulff, G. *Angew. Chem., Int. Ed. Engl.* **1995**, *34*, 1812–1832 and references therein. (b) Mosbach, K.; Ramstrom, O. *Biotechnology* **1996**, *14*, 163–170. (c) Shea, K. J. *Trends Polym. Sci.* **1994**, *A32*, 166–172. (d) *Molecular and Ionic Recognition with Imprinted Polymers*; ACS Symp. Ser. No. 703; Bartsch, R. A., Maeda, M., Eds.; American Chemical Society: Washington, DC, 1998.

(15) Sharma, A. C.; Borovik, A. S. *J. Am. Chem. Soc.* **2000**, *122*, 8946–8955.

(16) Perrin, D. D.; Armarego, W. L. F. *Purification of Laboratory Chemicals*, 3rd ed.; Pergamon Press: New York, 1988.

(17) Daly, J.; Horner, L.; Witkop, B. *J. Am. Chem. Soc.* **1961**, *83*, 4787–4792.

[CoI(dmap)₂][PF₆]. The following synthesis was conducted in the drybox under an argon atmosphere. To a 100-mL single-neck flask was added 0.991 g (1.86 mmol) of H₂I that was partially dissolved in 30 mL of 1,2-dichloroethane to give a yellow suspension. The purple methanolic (10 mL) Co(OAc)₂ (0.329 g, 1.86 mmol) solution was added to the suspension of the ligand with stirring. After addition was completed, the reaction mixture became orange in color and an orange precipitate began to form after approximately 5 min. 4-(Dimethylamino)pyridine, 0.455 g (3.72 mmol), in 10 mL of methanol, was then added to the mixture and no appreciable color change was observed. Ferrocenium hexafluorophosphate (0.616 g, 1.86 mmol) was partially dissolved in 30 mL of methanol to give a deep blue solution, which was then added to the reaction mixture. After approximately 1 h, the reaction mixture turned from the orange color to a deep red-brown. The reaction was then stirred for an additional 12 h after which volatile compounds were removed under reduced pressure to yield a brown solid. This solid was filtered and washed with diethyl ether until the diethyl ether became clear. The red-brown solid was then washed three times with a 3:1 diethyl ether:methanol solution and twice with diethyl ether. The solid was dried under vacuum overnight. Yield of the complex was 1.683 g (92%). Anal. Calcd for [CoI(dmap)₂][PF₆], C₄₈H₅₀CoF₆N₆O₄P: C, 58.90; H, 5.15; N, 8.59. Found: C, 58.93; H, 5.06; N, 8.25. ¹H NMR (CDCl₃): δ 7.88 (s, 2H, -N=CH(Ph)); 7.47 (d, 4H, *J* = 7 Hz, dmapH); 7.42 (m, 8H, styryl phenyl); 7.07 (d, 2H, *J* = 9 Hz, salicyl phenyl); 6.82 (d, 2H, *J* = 2 Hz, salicyl phenyl); 6.72 (dd, 2H, *J* = 11, 18 Hz, H(Ph)C=CH₂); 6.29 (d, 4H, *J* = 7 Hz, dmapH); 6.24 (dd, 2H, *J* = 9, 2 Hz, salicyl phenyl); 5.76 (d, 2H, *J* = 18 Hz, *trans*-H(Ph)C=CH₂); 5.26 (d, 2H, *J* = 11 Hz, *cis* H(Ph)C=CH₂); 5.02 (s, 4H, PhO-CH₂Ph); 4.01 (s, 4H, -CH₂CH₂-); 2.93 (s, 12H, dmap-NCH₃). IR (KBr): 3088 (w), 2924 (w), 2867 (w), 1625 (s), 1604 (s), 1527 (m), 1482 (w), 1430 (m), 1388 (m), 1306 (w), 1263 (w), 1226 (s), 1180 (m), 1143 (m), 1123 (m), 1063 (m), 1020 (m), 950 (w), 916 (w), 840 (bs) cm⁻¹. UV-vis (CH₂Cl₂, λ_{max}/nm (ε, M⁻¹ cm⁻¹)): 234 (56700), 271 (109000), 380 (11600). Mp 221–222 °C dec.

P-1[Co^{III}(dmap)₂]. All polymers were synthesized with 5 mol % of metal complex, 94 mol % of cross-linking agent, 1 mol % of initiator, and a 3:1 v/v ratio of porogenic agent to cross-linking agent. All reagents were added to a high-pressure glass reaction tube (Ace) and sealed with a screw cap under an argon atmosphere. The complex, [CoI(dmap)₂][PF₆] (0.660 g, 0.674 mmol), was added to the reaction tube and ~2/3 of the DMF (total DMF: 7.599 g, 104 mmol, 7.173 mL) was added. The remaining reagents were not added until the complex was completely dissolved. The ethylene glycol dimethacrylate (2.676 g, 13.5 mmol) and 2,2'-azobisisobutyronitrile (0.0235 g, 0.143 mmol) were then added using the remaining DMF. The tube was then sealed and the reaction mixture placed in an oil bath at ~60 °C for 24 h. After 24 h the DMF was removed under vacuum and the polymer was ground with a mortar and pestle. The ground polymer was placed in a Soxhlet apparatus and washed with methanol for 24 h. The resulting polymer was then dried under vacuum, ground, and sieved to a particle size of ≤75 μm. The yield of the red-brown polymer was 2.812 g. [Co] = 170–180 μmol of Co/g of polymer (range of values obtained). Nitrogen analysis: 1.64% found; 1.40% calculated; 1.61% calculated and corrected (the correction factor, 0.21%, is the average nitrogen content of three different samples of “complex-free” poly(EGDMA)). Fluoride analysis: 1.68% found; 1.89% calculated.

P-sal₂. The polymer P-1[Co^{III}(dmap)₂] (1.172 g) was treated with 50 mL of 0.1 M Na₂EDTA in deionized water. The reaction mixture was then refluxed for 24 h. The polymer was filtered and washed five times with 5-mL aliquots of deionized water, three times with methanol, and three times with diethyl ether. The polymer was then dried under vacuum. The yield of the resulting light tan polymer was 0.977 g. [Co] = 2–5 μmol of Co/g of polymer (range of values obtained). Nitrogen analysis: 0.17% found; 0.04% calculated; 0.25% calculated and corrected. Fluoride analysis: 0.05% found; 0.05% calculated.

P-1. The P-sal₂ polymer (1.127 g) was added to a 100-mL single-neck flask fitted with a septum. The polymer was degassed (three times) by successively applying a vacuum and refilling with nitrogen. To the flask was added 10 mL of freshly distilled methanol via syringe. One

equivalent of ethylenediamine (15.1 μL , 225 μmol , based on cobalt analysis of P-1[Co(dmap)₂][PF₆]) was added and the mixture was stirred for 6 h. The polymer was filtered and washed three times with diethyl ether and dried under vacuum for 15 min to yield 0.9413 g of a yellow-tan polymer. Nitrogen analysis: 0.76% found; 0.43% calculated; 0.64% calculated and corrected. [Co] = 3–6 μmol of Co/g of polymer (range of values obtained).

P-1[Co^{II}]. The polymer P-1 (0.901 g) was placed in a Schlenk tube and degassed by applying a vacuum and refilling with nitrogen three times. The polymer was then treated with 10 mL of a 0.1 M Co(OAc)₂ solution under an argon atmosphere. The mixture was stirred for 6 h. The polymer was then filtered into a fluted Whatman No. 41 (90 mm, ashless) filter paper and placed in a glass thimble (with coarse frit). The polymer was then washed in the Soxhlet apparatus with methanol for 14 h. The resulting polymer was dried under vacuum to yield 0.294 g of an orange-red polymer. [Co] = 170–230 μmol of Co/g of polymer (range of values obtained). The pore diameter was 25 Å.

Sample Preparation. UV–vis spectra of the monomeric compounds were obtained in solution with use of a 1.00-cm Suprasil quartz cell. Polymer samples for electronic absorbance spectroscopy were prepared by suspending the solid polymer in toluene under Ar in an anaerobic 1.00 cm quartz cell. Gaseous NO was added via syringe. Diffuse reflectance samples were 25% w/w mixture of polymer in KBr. Nitric oxide was added prior to mixing with KBr for these solid samples. EPR spectroscopy samples were prepared by placing approximately 20 mg of solid sample into a quartz EPR tube under argon atmosphere. Samples that required nitric oxide were packed under argon atmosphere and sealed, and gaseous NO was added via syringe.

Aluminum sample holders for X-ray absorption measurements were approximately 1 in. square by 1 mm thick and contained a 2 × 20 mm slit. The solid samples were packed dry under either an argon atmosphere (P-1[Co^{II}]) or an atmosphere of NO gas (P-1[Co(NO)]). Both samples were sealed with translucent electrical tape (3M#1205, Minneapolis, MN).

Physical Methods. All proton nuclear magnetic resonance (¹H NMR) spectra were collected on a 400-MHz Bruker spectrometer. Infrared spectra were collected on a Mattson Genesis Series FT-IR spectrometer. Solution and suspension UV–vis spectra were collected on a Cary 50 spectrophotometer. Diffuse reflectance spectra of the polymers were obtained on a SLM-Aminco 3000 diode array spectrophotometer equipped with a custom-made Harrick Scientific diffuse reflectance accessory (DRA-4). This system only allowed for data collection in the visible region of the spectrum (400–800 nm). Pore diameters and surface areas were determined with a Gemini surface area microanalyzer.

EPR spectra were collected with use of a Bruker EMX spectrometer equipped with an ER4102ST cavity. The instrument was previously calibrated with DPPH. Spectra for the Co^{II} samples were collected with use of the following spectrometer settings: attenuation = 25 dB, microwave power = 0.64 mW, frequency = 9.31 GHz, sweep width = 5000 G, modulation amplitude = 5.02 G, gain = 8.93 × 10⁻³, conversion time = 81.92 ms, time constant = 1.28 ms, and resolution = 1024 points.

X-ray absorption data were collected at the National Synchrotron Light Source at Brookhaven National Laboratory. Data for P-1[Co^{II}] was collected on beam line $\times 9\text{B}$ using a Si 220 monochromator low-angle nickel mirror for harmonic rejection and a closed-cycle helium cryostat to maintain sample temperature at ca. 25 K. P-1[Co(NO)] data were collected at room temperature on beam line $\times 18\text{B}$ using a Si 111 monochromator. Transmission spectra (including the cobalt foil calibration spectrum) were obtained with use of gas ionization chambers. The fluorescence spectra were obtained with 13-element Ge solid-state detectors (Canberra); a deadtime correction of 3 μs was used, but the effects of this were minimal since the total count rate was under 20000 s⁻¹ for each detector. Beam energy was calibrated by assigning the first inflection on the absorption edge of a cobalt foil to an energy of 7709.5 eV.¹⁹ The fluorescence mode XAS data were corrected for self-absorption and incident detector efficiency; transmission data were used in calculating the self-absorption correction.

Both transmission and fluorescence data were analyzed via general procedures described elsewhere using *Igor Pro* (Wavemetrics, Lake Oswego, OR) for data averaging and graphing.²⁰ Definitions of χ (EXAFS), k (the photoelectron wavenumber), and r' (the apparent Co–X distance in the Fourier transform) are in accord with general usage as established by Scott.²¹

The data for P-1[Co^{II}] and P-1[Co(NO)] from 7573 to 8465 eV (excluding the 7720–7741 eV region at the top of the edge rise) were fit to a cubic spline baseline with spline points at 7873 and 8173 eV; a small (<1%) K-edge from contaminating nickel was also removed as part of the baseline correction. After the baseline was fit, various analyses of the EXAFS region were performed. The best fit to the data was obtained by using a two-shell model (one N/O shell at ca. 2 Å and one C shell at ca. 2.8 Å). The program FEFF, version 7.0, was utilized during EXAFS analyses to obtain f and α as the average of functions calculated for Co–O and Co–N paths;²² E_0 was chosen as 7723 eV for the calculation of k .²³ The ionization potential for use with the f and α functions was refined in the fits (77.205 eV for P-1[Co^{II}] and 7721.5 eV for P-1[Co(NO)]). An amplitude reduction factor (S_0^2) of 0.85 (identical with that suggested for use in FEFF version 5)²⁴ was employed based on refinements of data from crystalline samples of Co(acac)₃, [Co(en)₃]Cl₃·H₂O, and [Co(NH₃)₆]Cl₃. In the reported fits the baselinge, edge, and EXAFS parameters were simultaneously refined to minimize the residual function $\text{gof} = [\sum\{\text{XAS-XAS}_{\text{calc}}/\text{esd}_{\text{data}}\}^2 / (\text{number of data} - \text{number of refined parameters})]^{1/2}$. The esd_{data} was taken to be 0.0005 below the edge and 0.05/ k^2 above the edge (this is equivalent to refining $k^2\chi$). The reported gof has been normalized to the refined edge height. The reported standard deviations were obtained from the *Igor Pro* least-squares analysis.

Determination of gas binding was accomplished by using a gas uptake apparatus, which is modeled after a system described by Taylor and co-workers.²⁵ The instrument consists of a series of chambers separated by Teflon-wetted solenoids (NR Research, West Caldwell, NJ). Five solenoids are used (Model 648T011, 12 V, two-way, normally closed, 3.9 mm orifice diameter, 2 atm pressure maximum) to create an upper (volume, 33.3 mL) and lower sample chamber (volume, 19.8 mL) and two gas-holding reservoirs. The apparatus utilizes a MKS Instruments absolute pressure transducer (Model 122BA-0500BB) interfaced to a MKS Type PDR-C-2C two-channel power supply/digital output device. All pressures are measured in units of Torr. The transducer is connected to a 316 stainless steel vacuum line (except where Teflon adapters have been used to convert the 1/8 in. straight threads of the solenoids to 1/8 in. NPT). The lower sample chamber assembly consists of a removable miniature sample cylinder (Nupro, 10 mL, 316 stainless steel). A removable 7- μm filter has been fitted directly above the sample cylinder to ensure that the samples do not enter the upper chamber. The two gas reservoirs have been designed to allow small quantities of gas into the system.

Samples were prepared as solids and placed in the sample chamber with a sample mass of 0.153 g. The sample chamber was then evacuated for a minimum of 30 min. Analyte gas (17 Torr of NO, CO₂, CO, or O₂) was introduced into the upper sample chamber while the lower sample chamber assembly remains under vacuum. When the lower sample chamber is opened and exposed to the analyte gas (system pressure now was at 10.3 Torr), pressure is recorded every 20 s until equilibrium is reached (typically 5 min). Data corresponding to changes in pressure were then converted to micromoles of analyte gas bound after accounting for the change in pressure that results from the increase in volume upon opening the sample chamber. Gas binding was measured for P-1[Co^{II}] ([Co^{II}] = 230 μmol of Co/g of polymer), P-1 ([Co^{II}] = 3.4 μmol of Co/g of polymer), the polymer without Co^{II} ions bonded to the immobilized sites, and poly(EGDMA), a porous polymer

(20) Scarrow, R. C.; Trimitsis, M. G.; Buck, C. P.; Grove, G. N.; Cowling, R. A.; Nelson, M. J. *Biochemistry* **1994**, *33*, 15023–15035.

(21) Scott, R. A. *Methods Enzymol.* **1985**, *117*, 414–459.

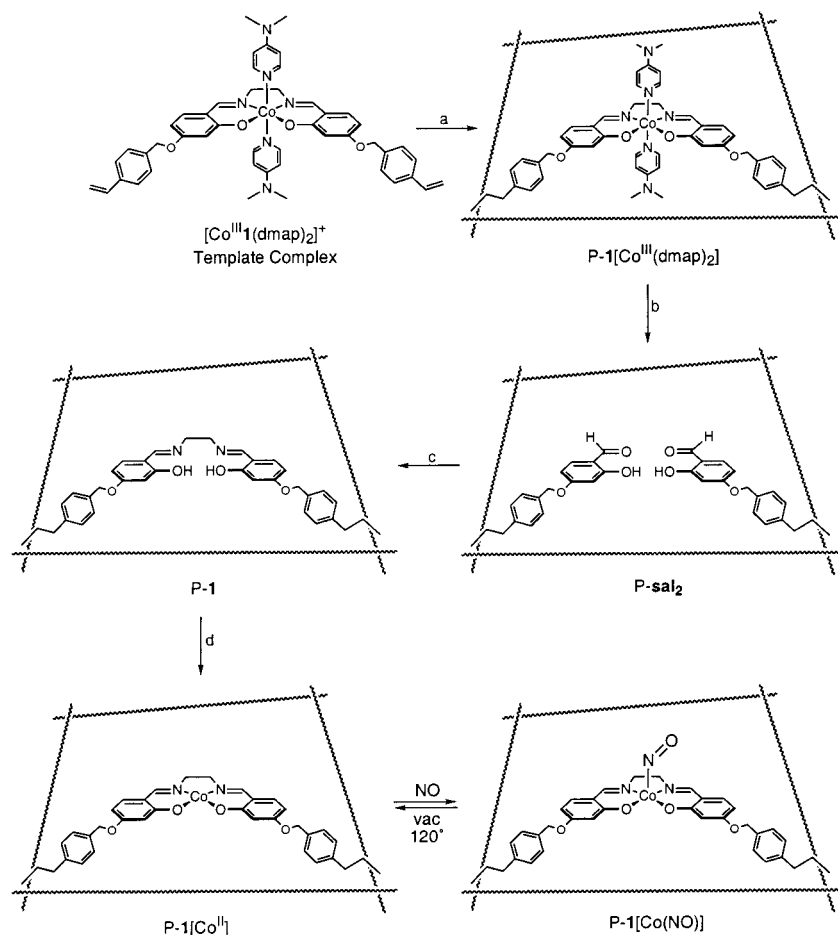
(22) Ankudinov, A. L.; Rehr, J. J. *Phys. Rev.* **1997**, *B56*, R1712–R1715.

(23) Brennan, B. A.; Alms, G.; Nelson, M. J.; Durney, L. T.; Scarrow, R. C. *J. Am. Chem. Soc.* **1996**, *118*, 9194–9195.

(24) O'Day, P. A.; Rehr, J. J.; Zabinsky, S. I.; Brown, G. E., Jr. *J. Am. Chem. Soc.* **1994**, *116*, 2938–2949.

(25) Taylor, R. J.; Drago, R. S.; George, J. E. *J. Am. Chem. Soc.* **1989**, *111*, 6610–6615.

(19) Bearden, J. A.; Burr, A. F. *Rev. Mod. Phys.* **1967**, *39*, 78–124.

Scheme 1^a

^a Conditions: a, EGDMA, AIBN, DMF, N₂, 60 °C; b, EDTA, H₂O, Δ; c, C₂H₈N₂, MeOH; d, Co(OAc)₂, MeOH, N₂.

without immobilized sites. Measurements were performed in triplicate; samples were evacuated for at least 10 min between trials where only nonselective physical adsorption is observed. In cases where chemical adsorption is observed, each measurement was made on new samples, which were thoroughly degassed prior to gas uptake. Gas uptake values for P-1[Co^{II}] have been corrected for nonselective physical adsorption by the polymer host. This was accomplished for each gas by subtracting the uptake data for P-1 from gas-binding data of P-1[Co^{II}].

Results and Discussion

Design and Synthesis of Polymers. The irreversible binding of NO to four-coordinate Co^{II} complexes is well documented.^{26,27} We have chosen one such complex, [Co^{II}(salen)] (salen, bis(2-hydroxy-benzaldehyde)ethylenediimine), to serve as the sites for NO binding in our polymeric material. In solution, monomeric [Co^{II}(salen)] forms a stable nitrosyl complex, [Co(salen)(NO)], under anaerobic conditions. In the presence of dioxygen, however, [Co(salen)(NO)] is unstable and is converted to the Co^{III}-nitrite complex, [Co^{III}(salen)(NO₂)]. It has been proposed that the formation of [Co^{III}(salen)(NO₂)] proceeds through the dimeric intermediate [(salen)Co^{III}(ON-O-O-NO)Co^{III}(salen)], which can readily form in solution at room temperature.²⁸ Immobilization of [Co(salen)(NO)] within

a porous polymeric host should allow for site isolation of the metal centers, thus preventing the bimolecular pathway leading to cobalt(III)-nitrite formation. With this pathway eliminated, the immobilized [Co(salen)(NO)] is stable within the polymeric host under ambient conditions. As a result, the composite material P-1[Co^{II}] can bind NO to form stable P-1[Co(NO)], which then functions as a storage material for nitric oxide. An advantage of this design is that subsequent removal of NO from P-1[Co(NO)] regenerates P-1[Co^{II}], which contains [Co^{II}(salen)] sites capable of rebinding additional NO molecules.

Scheme 1 represents the synthesis of P-1[Co^{II}] utilizing the general template copolymerization procedure for immobilization of metal complexes.^{12,13,15} This procedure utilizes a template complex (5 mol %), cross-linking agent (~95 mol %), and solvent, which serves as the porogen during the radical polymerization process. In the design of P-1[Co^{II}], the kinetically inert Co^{III} complex, [Co^{III}1(dmap)₂]⁺, is the template complex used to form the immobilized sites. This complex contains the styrene-modified salen ligand [1]²⁻,^{13,29} which is covalently attached to the porous methacrylate host by the procedure shown. To ensure that the metal complex is retained within the polymer host, two-point binding is utilized. P-1[Co^{III}(dmap)₂] typically has a cobalt concentration of between 170 and 180 μmol of Co/g of polymer with an average pore diameter of 25 Å. Note that immobilization of [Co^{III}1(dmap)₂]⁺ in a porous organic host with evidence of site isolation has been previously reported.¹²

(26) (a) Enemark, J. H.; Feltham, R. D. *Coord. Chem. Rev.* **1974**, *13*, 339–406. (b) Feltham, R. D.; Enemark, J. H. *Top. Stereochem.* **1981**, *12*, 155–215. (c) Richter-Addo, G. B.; Legzdins, P. *Metal Nitrosyls*; Oxford University Press: New York, 1992.

(27) Hoshino, M.; Konishi, R.; Tezuka, N.; Ueno, I.; Seki, H. *J. Phys. Chem.* **1996**, *100*, 13569–13574.

(28) Clarkson, S. G.; Basolo, F. *Inorg. Chem.* **1973**, *12*, 1528–1534.

(29) Fujii, Y.; Matsutani, K.; Kikuchi, K. *J. Chem. Soc., Chem. Commun.* **1985**, 415–417.

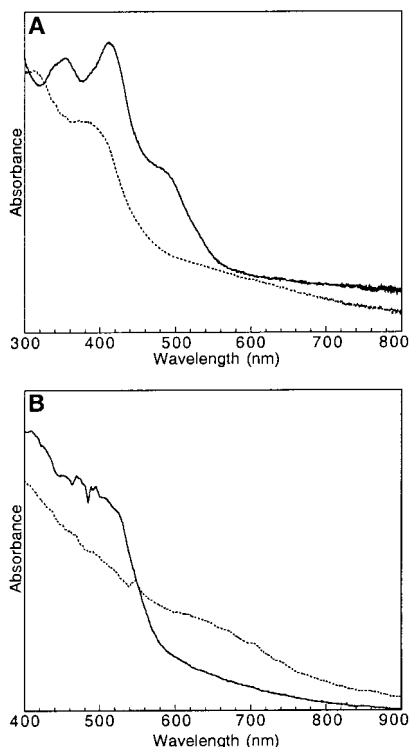


Figure 1. Electronic absorbance spectra for P-1[Co^{II}] (—) and P-1[Co(NO)] (---) (A) suspended in toluene and (B) solid-state diffuse reflectance spectra.

Once immobilized, the cobalt(III) ions and dmap ligands in P-1[Co^{III}(dmap)₂] are removed under acidic conditions to afford P-sal₂.³⁰ These conditions hydrolyze **1**, as is evident by the lack of nitrogen in the polymer and the characteristic salicylaldehyde $\nu(\text{C}=\text{O})$ at 1521 cm^{-1} . P-sal₂ contains immobilized sites with two salicylaldehyde moieties that are predisposed to bind ethylenediamine to reform the immobilized tetradentate salen ligand. The resulting polymer, P-1, readily binds Co^{II} ions to form P-1[Co^{II}], which contains immobilized four-coordinate Co^{II} centers. The cobalt concentration in P-1[Co^{II}] ranges from 180 to 230 μmol of Co/g of polymer with an average pore diameter of 25 Å.

Binding of NO to P-1[Co^{II}]. A. Electronic and EPR Spectral Properties. The absorbance spectra for suspensions of P-1[Co^{II}] and P-1[Co(NO)] in toluene are shown in Figure 1A.³¹ The absorbance spectrum of the P-1[Co^{II}] suspension has two bands at 350 and 410 nm with a shoulder centered at 495 nm. For P-1[Co(NO)], which was formed by treating the P-1[Co^{II}] suspension with gaseous NO, two prominent bands at 310 and 400 nm are observed. The spectrum of P-1[Co(NO)] also contains a weaker absorbance at ~ 600 nm. Note that the visible absorbance peaks of the monomeric complex, Co(salen) in ethanol, are at 353 and 415 nm and those of Co(salen)(NO) are at 410 and ~ 550 nm. The solid-state absorbance spectra for P-1[Co^{II}] and P-1[Co(NO)] are shown in Figure 1B and are qualitatively similar to those obtained as suspensions. The diffuse reflectance visible spectrum of P-1[Co^{II}] in KBr has a shoulder centered at 500 nm. The tail of the stronger absorbance band, originating from the UV region, is also observed. The diffuse reflectance visible absorbance spectrum of P-1[Co(NO)] has a feature at ~ 650 nm; the 500-nm shoulder found in P-1[Co^{II}] is absent in the spectrum of P-1[Co(NO)].

(30) Attempts to reduce the cobalt centers with ascorbic acid or dithionite are not as efficient in removing the cobalt and dmap as that described.

(31) P-1[Co^{II}] and P-1[Co(NO)] suspensions in toluene produce optically transparent mixtures.



Figure 2. Observed colors of polymers: P-1[Co^{II}] (top) and P-1[Co(NO)] (bottom).

The differences in the absorbance properties of P-1[Co^{II}] and P-1[Co(NO)] lead to striking color changes in these materials. This color conversion is shown in Figure 2. In the presence of NO, the orange P-1[Co^{II}] changes to the brown-green P-1[Co(NO)] polymer. The conversion back to the orange P-1[Co^{II}] is accomplished in ~ 1 h when P-1[Co(NO)] is heated to 120 °C under vacuum (0.05 Torr). Note that porous poly(EGDMA) without immobilized Co^{II}(salen) sites remains colorless in the presence of NO.

The reversible binding of NO to P-1[Co^{II}] can also be observed by EPR spectroscopy. The immobilized low-spin Co^{II}(salen) complexes in P-1[Co^{II}] are EPR active with signals originating from the $\pm 1/2$ doublet ground state. Figure 3A shows the X-band EPR spectrum of solid P-1[Co^{II}] measured at 77 K. An axial spectrum is obtained with g -values at 3.83 and 1.98. This spectrum is consistent with a square-planar coordination geometry about the Co^{II} ions. Addition of NO to form P-1[Co(NO)] quenches the EPR signal. The lack of signal for P-1[Co(NO)] is consistent with the immobilized metal centers being diamagnetic, which could result from antiferromagnetic coupling of the unpaired electrons on NO and the Co center.³² Removal of NO from P-1[Co(NO)] by heating under vacuum (vide supra) affords the axial EPR signal of P-1[Co^{II}]. The immobilized cobalt sites in this regenerated form of P-1[Co^{II}] are still capable of binding NO as shown by the quenching of the axial EPR signal upon the addition of NO. Under conditions of room temperature and pressure, 40% conversion of P-1[Co(NO)] to P-1[Co^{II}] is observed within 14 d, as determined by comparison of the relative areas of the collected EPR signals (Figure 3B).

Similar EPR properties are observed for suspensions of P-1[Co^{II}] and P-1[Co(NO)] in noncoordinating solvents. For example, suspensions of P-1[Co^{II}] and P-1[Co(NO)] in toluene give identical spectra to those measured in the solid state. More complicated EPR spectra are obtained for suspensions of P-1[Co^{II}] in coordinating solvents, such as water and methanol.

(32) (a) Earnshaw, A.; Hewlett, P. C.; Larkworthy, L. F. *J. Chem. Soc.* **1965**, 4718–4723. (b) Earnshaw, A.; Hewlett, P. C.; King, E. A.; Larkworthy, L. F. *J. Chem. Soc.* **1968**, 241–246. (c) Duffin, P. A.; Larkworthy, L. F.; Mason, J.; Stephen, A. N.; Thompson, R. M. *Inorg. Chem.* **1987**, 26, 2034–2040.

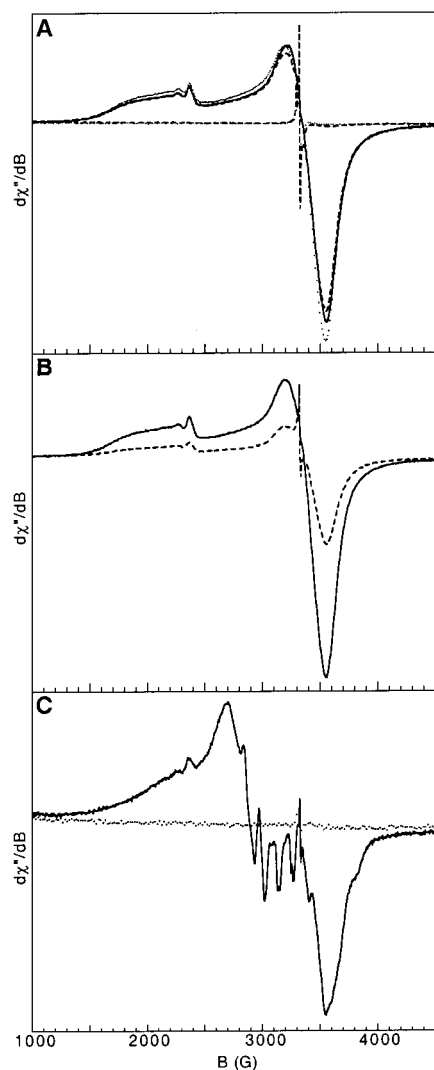


Figure 3. (A) X-band EPR spectra measured at 77 K for two complete cycles of NO addition to solid P-1[Co^{II}] and subsequent removal at 120 °C under vacuum (total of five spectra reported): initially recorded spectrum of P-1[Co^{II}] (—), first addition and removal cycle (···), and second NO addition and removal cycle for P-1[Co(NO)] (---). Note that for each cycle there are two spectra, one showing the quenching of the signal after NO addition and the second the axial signal after NO removal. (B) X-band EPR spectra measured at 77 K for solid P-1[Co^{II}] (—) and P-1[Co(NO)] after exposure to room temperature and pressure for 14 d (---). (C) X-band EPR spectra measured at 77 K for a water suspension of P-1[Co^{II}] (—) and after treating the polymer with NO (---).

Figure 3C shows the EPR spectrum of P-1[Co^{II}] suspended in water. The spectrum suggests that water molecule(s) have coordinated to some of the immobilized Co^{II} centers. This EPR signal is completely quenched when NO is added to the suspension, indicating that the immobilized sites are capable of binding NO in an aqueous medium.

The spectral properties of P-1[Co^{II}] and P-1[Co(NO)] are nearly identical with those reported for monomeric Co^{II}(salen) and Co(salen)(NO) complexes in solution.²⁷ This indicates that the coordination geometries of the immobilized cobalt complexes in the polymeric hosts are similar to those of their molecular analogues. However, immobilization of Co^{II}(salen) complexes in a porous host has a dramatic effect on the binding of NO to the cobalt centers. The reversible binding of NO observed for P-1[Co^{II}] contrasts the irreversible binding reported for monomeric Co^{II}(salen) in solution and the solid state.²⁷ In

addition, the Co–NO sites in P-1[Co(NO)] are stable in the presence of O₂, whereas in solution Co(salen)(NO) complexes are unstable and form (salen)Co^{III}–NO₂ complexes.²⁸ The difference in Co–NO stability can be explained by the site isolation properties provided by the organic host in P-1[Co^{II}]. As a result, the formation of dimeric cobalt species, essential for the formation of the Co^{III}–NO₂ complexes, is prevented and removal of NO from the polymer is possible.

B. X-ray Absorption Spectroscopy. The cobalt K-edge X-ray absorption spectra (XAS) of P-1[Co^{II}] and P-1[Co(NO)] were measured to further investigate the geometric properties of the immobilized cobalt sites. X-ray absorption near edge structure (XANES) spectra and extended X-ray absorption fine structure (EXAFS) were obtained for frozen samples of solid P-1[Co^{II}] and P-1[Co(NO)]. Figure 4a shows the XANES spectra for P-1[Co^{II}] and P-1[Co(NO)], which have edge positions of 7719.48(2) and 7720.86(2) eV, respectively. The lowest energy preedge peak in each spectrum is assigned to the 1s → 3d transition. The area of this peak is sensitive to the symmetry of the cobalt complexes, and thus can be used to probe the coordination number and geometry of the cobalt centers. For P-1[Co^{II}], the 1s → 3d preedge peak is found at 7709.9(1) eV with a refined area/edge height of 0.06(1) eV, while that for P-1[Co(NO)] occurs at 7710.47(1) eV with a refined area/edge height of 0.220(3) eV (Figure 4b). The relatively small value for the area of the 1s → 3d peak in P-1[Co^{II}] indicates that its cobalt centers are centrosymmetric. A square-planar coordination geometry for the immobilized cobalt centers is consistent with this symmetry requirement. Support for this assignment is provided by the large shoulder (area/edge height of 0.32 eV) observed at 7715.30(2) eV, which is attributed to the 1s → 4p_z transition.³³ In contrast, the significantly larger area observed for the 1s → 3d preedge peak in P-1[Co(NO)] is consistent with a loss of centrosymmetry caused by the formation of a five-coordinate complex in the presence of NO. The loss of centrosymmetry allows mixing between the 3d and 4p orbitals, which results in area increases of the 1s → 3d preedge peak.

The results of EXAFS spectral analysis for P-1[Co^{II}] and P-1[Co(NO)] (Figure 5) support the coordination changes proposed between the two polymers and the direct binding of NO to the immobilized cobalt centers. The best fit of the EXAFS data for P-1[Co^{II}] gives 3.7(2) nitrogen and/or oxygen ligands bonded to the Co^{II} centers at a distance of 1.859(4) Å. These metrical values are in agreement with those reported from X-ray diffraction studies of molecular square planar Co^{II} complexes with similar tetradentate ligands. For example, the average Co–N/O bond distance in Co^{II}salen·CHCl₃ is 1.849(6) Å.³⁴ The EXAFS analysis for P-1[Co(NO)] indicates that the cobalt centers have increased their coordination number by 20%; the refined number being 4.6(1). The average Co–N/O bond distance in P-1[Co(NO)] is 1.886(2) Å, which is similar to the 1.862(2) Å average bond distance found for [Co(salen)(NO)] by X-ray diffraction methods.³⁵

C. Gas Uptake Measurements. The immobilized sites in P-1[Co^{II}] selectively bind NO relative to the biologically important gases O₂, CO₂, and CO. This selectivity is demonstrated by gas uptake measurements, results of which are shown

(33) This assignment is made based on analogy to peaks found in square-planar Ni^{II} complexes: Colpas, G. J.; Maroney, M. J.; Bagyinka, C.; Kumar, M.; Willis, W. S.; Suib, S. L.; Baidya, N.; Mascharak, P. K. *Inorg. Chem.* **1991**, *30*, 920–928.

(34) Schaefer, W. P.; March, R. E. *Acta Crystallogr.* **1969**, *B25*, 1675–1682.

(35) Haller, K. J.; Enemark, J. H. *Acta Crystallogr.* **1978**, *B34*, 102–109.

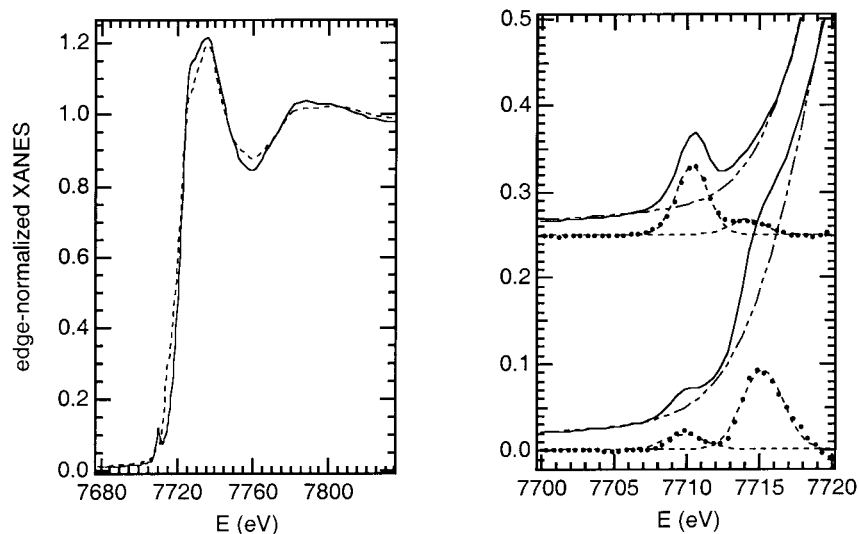


Figure 4. (Left) Comparison of XANES spectra for solid P-1[Co(NO)] (—) and P-1[Co^{II}] (---). (Right) Comparison of preedges of solid P-1[Co(NO)] (top: offset by +0.25) and solid P-1[Co^{II}] (bottom: no offset). Five plots are presented for each polymer: the measured preedge data with baseline subtracted and normalized to the edge height (—), the fits to the edge by the integral of a 75% Gaussian/25% Lorentzian peak (— · —), the difference when the edge fit is subtracted from the data (···), and the deconvolution of the preedge peaks into two Gaussian peaks of the same width (---).

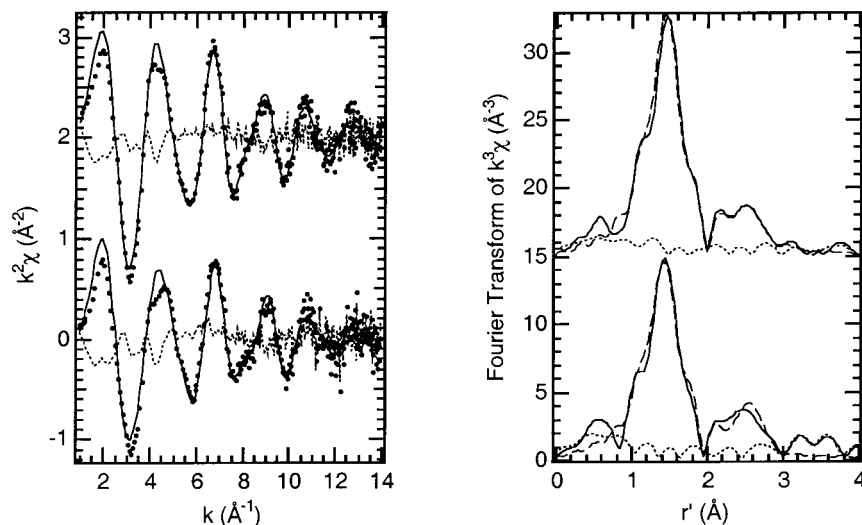


Figure 5. (Left) EXAFS ($k^2\chi$) of solid P-1[Co(NO)] (top: offset by +2) and solid P-1[Co^{II}] (no offset). EXAFS data are shown by circles, solid lines represent the computer generated fits, and the difference is shown with dots. (Right) Comparison of Fourier filtered $k^3\chi$ (data from $k = 1-14$ Å⁻¹ are filtered with a 5% window). Solid lines are Fourier transforms (FT) of data, dashed lines are FT of the fits, and dotted lines are FT of the residual from the fits. The top shows P-1[Co^{II}(NO)], and the bottom shows P-1[Co^{II}].

in Figure 6. Solid samples of P-1[Co^{II}] were exposed to 10.3 Torr (30.5 μ mol) of gas and uptake was monitored as a change in pressure with respect to time. The uptake data presented in Figure 6A indicate that the cobalt sites in P-1[Co^{II}] bound 21 μ mol of NO within 2 min. This accounts for a 70% uptake of the available NO, which corresponds to 60% of the immobilized cobalt sites binding NO. In contrast, the immobilized Co^{II} sites in P-1[Co^{II}] display no detectable affinity for O₂, CO₂, and CO when exposed to 30.5 μ mol of each gas (Figure 6A).³⁶ The importance of the Co^{II} ions in the NO binding process was examined by gas uptake to the apo polymer, P-1, a polymer without Co^{II} ions coordinated to the immobilized salen sites (Scheme 1). P-1 takes up only ~ 3 μ mol of NO; similar results were obtained for the uptake of O₂, CO₂, and CO to P-1 (Figure 6B). The gas uptake values for P-1 are nearly identical with

those obtained for solid poly(EGDMA),¹⁵ a porous polymer without immobilized sites (Figure S1). These results establish that for P-1, only nonselective physical adsorption of gas is occurring, and that intact Co^{II}(salen) sites are necessary for selective binding of NO in these polymers.

These findings are consistent with the binding properties reported for similar square-planar Co^{II} complexes. Square-planar Co^{II}salen complexes are very weak binders of O₂; a change in the cobalt coordination geometry to square pyramidal is needed to allow O₂ to bind at an appreciable level.^{13,15,37} The low binding affinity of P-1[Co^{II}] for CO₂ and CO is also consistent with the binding properties reported for other monomeric analogues,³⁸ where square-planar Co^{II} complexes weakly bind these two gases.

(36) These values are corrected for physical gas adsorption. See the legend in Figure 6 and Experimental Section for details.

(37) (a) Cesarotti, E.; Gullotti, M.; Pasini, A.; Ugo, R. *J. Chem. Soc., Dalton Trans.* **1977**, 757–763. (b) Meier, I. K.; Pearlstein, R. M.; Ramprasad, D.; Pez, G. P. *Inorg. Chem.* **1997**, *36*, 1707–1714 and references therein.

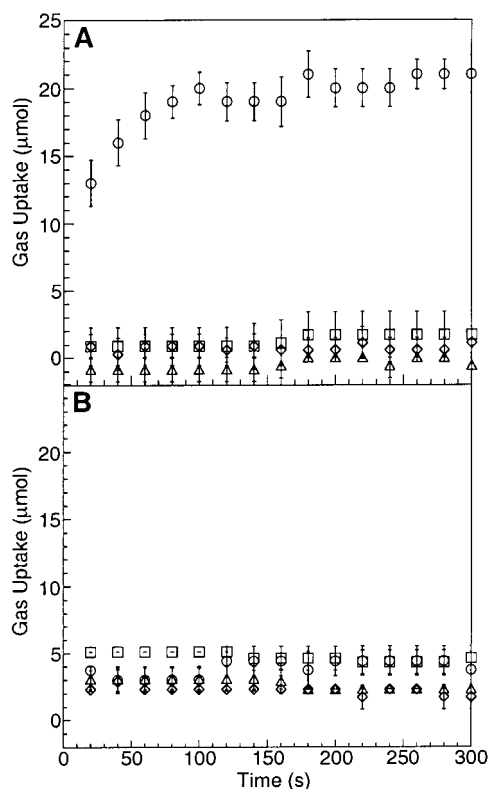


Figure 6. Gas binding versus time for P-1[Co^{II}] (A) and P-1 (B). Legend of analyte gases: NO (○), O₂ (△), CO₂ (□), and CO (◇). The gas uptake plots in part A have been corrected for physical adsorption by subtracting the values of P-1 binding from those of P-1[Co^{II}] for each gas, respectively.

Summary and Conclusions. Immobilization of metal complexes in porous organic hosts from soluble molecular precursors has proven to be an effective way of generating new functional materials. The results presented in this paper demonstrate the usefulness of this approach in developing a polymer for the storage and release of NO. Spectroscopic measurements show that the Co^{II}(salen) complexes can be immobilized within a porous polymethacrylate host and serve as sites for NO binding. The Co^{II}(salen) polymer, P-1[Co^{II}], binds NO but is relatively inert toward other biologically important gaseous compounds such as O₂, CO₂, and CO. Nitric oxide is slowly released from P-1[Co(NO)] under ambient conditions; ~80% of NO is lost from P-1[Co(NO)] after 30 days. The slow release of NO as observed for P-1[Co(NO)] is advantageous for certain applications, such as the prevention of restenosis after angioplasty.³⁹

The NO binding properties of P-1[Co^{II}] and P-1[Co(NO)] contrast those found for their molecular analogues. This

(38) Buckingham, D. A.; Clark, C. R. In *Comprehensive Coordination Chemistry*; Wilkinson, G., Gillard, R. D., McCleverty, J. A., Eds.; Pergamon Press: New York, 1987; Vol. 4, pp 635–900. Sweany, R. L. In *Comprehensive Organometallic Chemistry II*; Abel, E. W., Stone, F. G. A., Wilkinson, G., Eds.; Pergamon Press: New York, 1995; Vol. 8, p 8.

difference is attributed to the presence of the porous poly-methacrylate host in these materials. The ability of the host to isolate the metal sites from each other leads to different reactivity than is observed for the corresponding monomers. Similar types of results have been obtained for dioxygen binding polymers made by template copolymerization methods.^{13,15} These results highlight the importance of the immobilization process in tuning metal ion reactivity.

The vivid color change resulting from the conversion of P-1[Co^{II}] to P-1[Co(NO)] suggests the potential of this system for the detection of NO. Numerous methods are available for detecting NO;^{40,41} however, most do not directly detect NO but rather, sense adducts including NO₂. In addition, few of the methods reported to date are as durable as the highly cross-linked polymer, P-1[Co^{II}]. This polymer can be recycled, retaining high binding affinity for NO, and functions equally well in the solid state or as a suspension in a liquid. These properties lend this system to use in a variety of detection applications and efforts to incorporate materials of this kind into sensor technology are ongoing.

Acknowledgment. We thank K. Trafford for assistance in collecting the XAS data and Professor C. Loudon for helpful discussions. Financial support of this work was provided by ONR-DEPSCoR and NIH. The Bruker EMX-EPR spectrometer was purchased with funds obtained from the ONR-DURIP program.

Supporting Information Available: Table of XAS parameters (Table S1) and gas uptake to poly(EGDMA) (Figure S1) (PDF). This material is available free of charge via the Internet at <http://pubs.acs.org>.

JA003282B

(39) Smith, D. J.; Chakravarthy, D.; Pulfer, S.; Simmons, M. L.; Hrabie, J. A.; Citro, M. L.; Saavedra, J. E.; Davies, K. M.; Hutsell, T. C.; Mooradian, D. L.; Hanson, S. R.; Keefer, L. K. *J. Med. Chem.* **1996**, *39*, 1148–1156.

(40) Selected references. Spectrophotometric: Green, L. C.; Wagner, D. A.; Glogowski, J.; Skipper, P. L.; Wishnok, J. S.; Tannenbaum, S. R. *Anal. Biochem.* **1982**, *126*, 131–138. Luminescence methods: Kikuchi, K.; Nagano, T.; Hayakawa, H.; Hirata, Y.; Hirobe, M. *Anal. Chem.* **1993**, *65*, 1794–1799. Leone, A. M.; Furst, V. W.; Foxwell, N. A.; Cellek, S.; Moncada, S. *Biochem. Biophys. Res. Commun.* **1996**, *221*, 37–41. Zhou, X.; Arnold, M. A. *Anal. Chem.* **1996**, *68*, 1748–1754. Kojima, H.; Nakatsubo, N.; Kikuchi, K.; Kawahara, S.; Kirino, Y.; Nagoshi, H.; Hirata, Y.; Nagano, T. *Anal. Chem.* **1998**, *70*, 2446–2453. Barker, S. L. R.; Zhao, Y.; Marletta, M. A.; Kopelman, R. *Anal. Chem.* **1999**, *71*, 2071–2075. Electrochemical methods: Malinski, T.; Taha, Z. *Nature* **1992**, *358*, 676–677. Pariente, F.; Alonso, J. L.; Abruña, H. D. *J. Electroanal. Chem.* **1994**, *379*, 191–197. Friedemann, M. N.; Robinson, S. W.; Gerhardt, G. A. *Anal. Chem.* **1996**, *68*, 2621–2628. Maskus, M.; Pariente, F.; Wu, Q.; Toffanin, A.; Shapleigh, J. P.; Abruña, H. D. *Anal. Chem.* **1996**, *68*, 3128–3134. Mitchell, K. M.; Michaelis, E. K. *Electroanalysis* **1998**, *10*, 81–88. EPR spectroscopy: Yoshimura, T.; Yokoyama, H.; Fujii, S.; Takayama, F.; Oikawa, K.; Kamada, H. *Nature Biotech.* **1996**, *14*, 992–994.

(41) For recent examples of molecular systems that induce spectral changes upon NO binding see: (a) Franz, K. J.; Singh, N.; Lippard, S. J. *Angew. Chem., Int. Ed. Engl.* **2000**, *39*, 2120–2122. (b) Rathore, R.; Lindeman, S. V.; Rao, K. S. S. P.; Sun, D.; Kochi, J. K. *Angew. Chem., Int. Ed. Engl.* **2000**, *39*, 2123–2127.